SNRs W28 and W44: old cosmic ray accelerators in molecular clouds

V.N.Zirakashvili, V.S.Ptuskin
Pushkov Institute of Terrestrial Magnetism, Ionosphere and Radiowave Propagation, 108840 Moscow Troitsk, Russia

Nonlinear model of diffusive shock acceleration is used for investigation of the particle acceleration in old supernova remnants W28 and W44. We modeled the hydrodynamical evolution of the remnants, shock modification and streaming instability produced by accelerated particles. Comparison with available radio and gamma-ray data is given.

arXiv:1701.00844v3 [astro-ph.HE] 15 Jan 2017

I. INTRODUCTION

The diffusive shock acceleration (DSA) process [1–4] is considered as the principal mechanism for production of galactic cosmic rays (CR) in supernova remnants (SNRs). During the last decade the excellent results of X-ray and gamma-ray astronomy supplied the observational evidence of the presence of multi-TeV energetic particles in these objects (see e.g. [5]).

Most of existing DSA models were applied to young SNRs (see however [6]). This is probably because it is expected that CRs with highest energies are produced there. However lower energy particles are produced in old SNRs either. So the investigation of CR acceleration in old SNRs is important for calculation of overall CR spectra produced by SNRs.

In this paper we describe the modifications of our non-linear DSA model [7] designed for investigation of DSA in old SNRs. We apply it for two GeV bright old SNRs W28 and W44.

II. NONLINEAR DIFFUSIVE SHOCK ACCELERATION MODEL

Details of our model of nonlinear DSA can be found in [7]. The model contains coupled spherically symmetric hydrodynamic equations and the transport equations for energetic protons, ions and electrons. The forward and reverse shocks are included in the consideration.

Damping of magnetohydrodynamic (MHD) waves due to the presence of neutral atoms is important for old SNRs. To take this effect into account we add the equation that describes the transport and generation of MHD waves (see Eq.(4) below).

The hydrodynamical equations for the gas density $\rho(r,t)$, gas velocity $u(r,t)$, gas pressure $P_g(r,t)$, wave pressure $P_m(r,t)$, and the equation for isotropic part of the cosmic ray proton momentum distribution $N(r,t,p)$ in the spherically symmetrical case are given by

$$\frac{\partial \rho}{\partial t} = -\frac{1}{r^2}\frac{\partial}{\partial r} r^2 u \rho \qquad (1)$$

$$\frac{\partial u}{\partial t} = -u\frac{\partial u}{\partial r} - \frac{1}{\rho}\left(\frac{\partial P_g}{\partial r} + \frac{\partial P_c}{\partial r} + \frac{\partial P_m}{\partial r}\right) \qquad (2)$$

$$\frac{1}{\gamma_g - 1}\left(\frac{\partial P_g}{\partial t} + u\frac{\partial P_g}{\partial r} + \frac{\gamma_g P_g}{r^2}\frac{\partial r^2 u}{\partial r}\right) = -\Lambda(T_e)n^2 + H_c + 2\Gamma_n \frac{P_m}{\gamma_m - 1} - \xi_A V_{Ar}(1-h_m)\frac{\partial P_c}{\partial r} \qquad (3)$$

$$\frac{\partial P_m}{\partial t} + (u + \xi_A V_{Ar})\frac{\partial P_m}{\partial r} + \frac{P_m}{r^2}\frac{\partial r^2(\gamma_m u + \xi_A V_{Ar})}{\partial r} = -h_m(\gamma_m - 1)\xi_A V_{Ar}\frac{\partial P_c}{\partial r} - 2\Gamma_n P_m \qquad (4)$$

$$\frac{\partial N}{\partial t} = \frac{1}{r^2}\frac{\partial}{\partial r} r^2 D(p,r,t)\frac{\partial N}{\partial r} - w\frac{\partial N}{\partial r} + \frac{\partial N}{\partial p}\frac{p}{3r^2}\frac{\partial r^2 w}{\partial r} + \frac{1}{p^2}\frac{\partial}{\partial p} p^2 b(p) N + \frac{\eta_f \delta(p-p_f)}{4\pi p_f^2 m}\rho(R_f+0,t)(\dot{R}_f - u(R_f+0,t))\delta(r-R_f(t)) + \frac{\eta_b \delta(p-p_b)}{4\pi p_b^2 m}\rho(R_b-0,t)(u(R_b-0,t) - \dot{R}_b)\delta(r-R_b(t)) \qquad (5)$$

Here $P_c = 4\pi \int dp p^3 v N/3$ is the cosmic ray pressure, $w(r,t)$ is the advection velocity of cosmic rays, T_e, γ_g and n are the gas temperature, adiabatic index and number density respectively, γ_m is the wave adiabatic index, $D(r,t,p)$ is the cosmic ray diffusion coefficient. The radiative cooling of gas is described by the cooling function $\Lambda(T_e)$. The function $b(p)$ describes the energy losses of particles. In particular the Coulomb losses of sub GeV ions and the radiative cooling are important in old SNRs. The energy of sub GeV ions goes to the gas heating described by the term H_c in Eq. (3).

Cosmic ray diffusion is determined by particle scattering on magnetic inhomogeneities. The cosmic ray streaming instability increases the level of MHD turbulence in the shock vicinity [2] and even significantly amplifies the absolute value of magnetic field in young SNRs [8, 9]. It decreases the diffusion coefficient and increases the maximum energy of accelerated particles. The results of continuing theoretical study of this effect can be found in review papers [10, 11].

Cosmic ray particles are scattered by moving waves and it is why the cosmic ray advection velocity w may differ from the gas velocity u by the value of the radial component of the Alfvén velocity $V_{Ar} = V_A/\sqrt{3}$ calculated in the isotropic random magnetic field: $w = u + \xi_A V_{Ar}$. The factor ξ_A describes the possible deviation of the cosmic ray drift velocity from the gas velocity. We use values $\xi_A = 1$ and $\xi_A = -1$ upstream of the forward and reverse shocks respectively, where Alfvén waves are generated by the cosmic ray streaming instability and propagate in the corresponding directions.

The pressure of generated waves P_m determines the scattering and diffusion of energetic particles with charge q, momentum p and speed v

$$D = D_B \frac{B^2}{8\pi P_m},\ D_B = \frac{cpv}{3qB},\ B = \sqrt{B_0^2 + 8\pi P_m} \quad (6)$$

where B is the total magnetic field strength, while B_0 is the strength of the mean field. At high wave amplitudes the diffusion coefficient coincides with the Bohm diffusion coefficient D_B.

The parameter h_m in Eqs. (3,4) describes the fraction of magnetic energy produced by streaming instability. We use the following dependence $h_m(B)$

$$h_m = 1,\ \frac{B}{B_0} < 3;\ h_m = 0.5,\ \frac{B}{B_0} > 3. \quad (7)$$

At high amplitudes the waves are damped and the fraction $1 - h_m$ of energy goes into the gas heating upstream of the shocks [12] that is described by the last term in Eq. (3). The heating and wave generation limits the total compression ratio of cosmic ray modified shocks. In the downstream region of the forward and reverse shock at $R_b < r < R_f$ we put $\xi_A = 0$ and therefore $w = u$.

In the shock transition region the magnetic pressure is increased by a factor of σ^{γ_m}, where σ is the shock compression ratio. Its impact on the shock dynamics is taken into account via the Hugoniot conditions.

Below we use the adiabatic index of Alfvén waves $\gamma_m = 3/2$. For this value of the adiabatic index, the wave pressure $P_m = (\delta B)^2/8\pi$ equals to the wave magnetic energy density.

The rate of the neutral damping $\Gamma_n = 0.5\sigma_{ex} \mathrm{v}_T n_n$ depends on the number density of neutrals n_n, thermal speed $\mathrm{v}_T \sim 10$ km s^{-1} and charge exchange cross-section $\sigma_{ex} \sim 10^{-14}$ cm^2. We take the damping into account in the upstream region only and put $\Gamma_n = 0$ downstream of the shock.

Two last terms in Eq. (5) correspond to the injection of thermal protons with momenta $p = p_f$, $p = p_b$ and mass m at the forward and reverse shocks located at $r = R_f(t)$ and $r = R_b(t)$ respectively . The dimensionless parameters η_f and η_b determine the efficiency of injection.

TABLE I: Physical parameters of SNRs W28 and W44

	d	R_f	E_{SN}	M_{ej}	n_H	n_n	K_{ep}	T	V_f	B_f
	kpc	pc	10^{51}erg	$M_\odot$	cm^{-3}	cm^{-3}		kyr	km/s	μG
W28	1.9	13.4	1.3	6.8	4.0	0.2	0.008	37	121	79
W44	2.8	12.4	1.6	7.1	6.0	0.3	0.006	33	130	102

The injection efficiency is taken to be independent of time $\eta_f = 0.001$, and the particle injection momentum is $p_f = 2m(\dot{R}_f - u(R_f + 0, t))$. Protons of mass m are injected at the forward shock. The high injection efficiency results in the significant shock modification already at early stage of SNR expansion. Since in the old remnants the reverse shock absent we put $\eta_b = 0$ in the modeling below.

We neglect the pressure of energetic electrons and treat them as test particles. The evolution of the electron distribution is described by equation analogous to Eq. (5) with function $b(p)$ describing Coulomb, synchrotron and inverse Compton (IC) losses and additional terms describing the production of secondary leptons by energetic protons and nuclei.

III. MODELING OF DIFFUSIVE SHOCK ACCELERATION IN THE OLD SNRS

A significant part of core collapse supernova explosion occurs in molecular gas. The stars with initial masses below 12 $M_\odot$ have no power stellar winds and therefore do not produce a strong modification of their circumstellar medium. The molecular cloud have been totally destroyed by stellar winds and supernova explosions of more massive stars at the instant of explosion. As a result the star explodes in the inter-clump medium with the density $5 - 25$ cm^{-3} [13]. Many such SNRs are observed in gamma rays now.

Bright in GeV gamma rays SNRs W44 and W28 at distance $d \sim 2 - 3$ kpc from the Earth are at the radiative phase now and show signs of interaction with molecular gas [14]. It is believed that circumstellar medium is almost fully ionized by ultraviolet radiation from the remnant interior at the radiative stage [13]. The same is true for young SNRs because the gas is ionized by the radiation from the shock breakout and in the hot shock precursor produced by accelerated particles. Probably there exist an intermediate phase when the shock propagates in the neutral medium. We leave the detail description of the gas ionization to the future work. Here we shall use a simplified approach and consider the number density of neutrals n_n as a free parameter.

The parameters of supernova modeling are given in Table I. The explosion energy E_{SN} was taken within the range $(1 - 2) \cdot 10^{51}$ erg. The ambient number

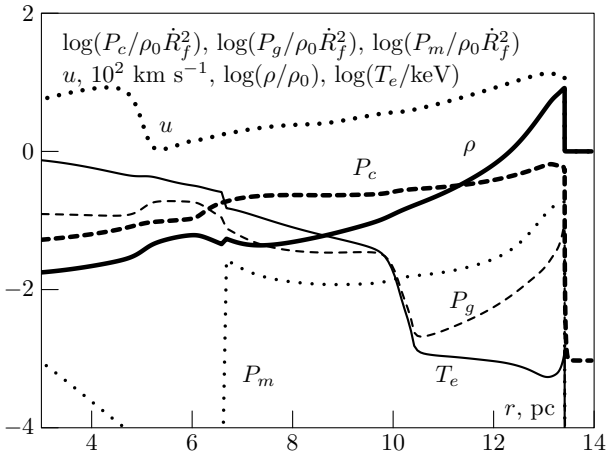


FIG. 1: Radial dependencies of the gas density (thick solid line), the gas velocity (dotted line), CR pressure (thick dashed line), the wave magnetic energy density $(\delta B)^2/8\pi = P_m$ (thin dotted line), the gas temperature T_e (thin solid line) and the gas pressure P_g (dashed line) at $T = 37$ kyr in SNR W28.

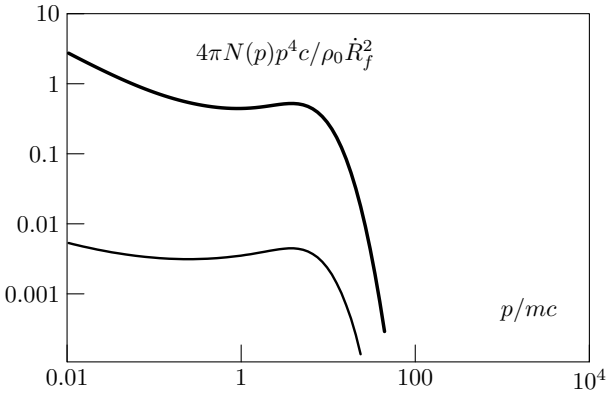


FIG. 2: Spectra of accelerated particles at the forward shock in SNR W28 at $T = 37$ kyr. The spectrum of protons (thick solid line) and electrons (thin solid line) are shown.

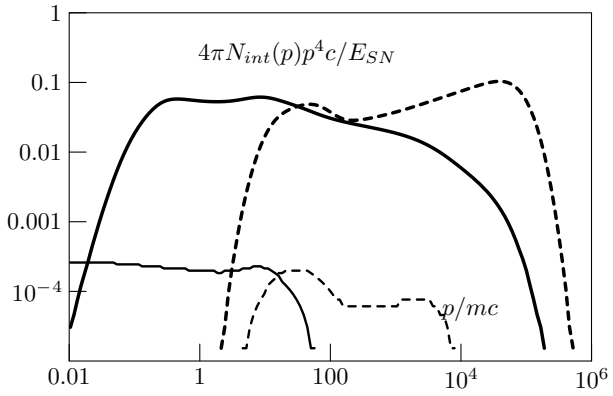


FIG. 3: Spectra of particles produced in the SNR W28 during 37 kyr after explosion. The spatially integrated spectrum of protons (thick solid line), the spectrum of protons escaped from the remnant (dashed line), the integrated spectrum of electrons (thin solid line) and the spectrum of electrons escaped from the remnant (thin dashed line) are shown.

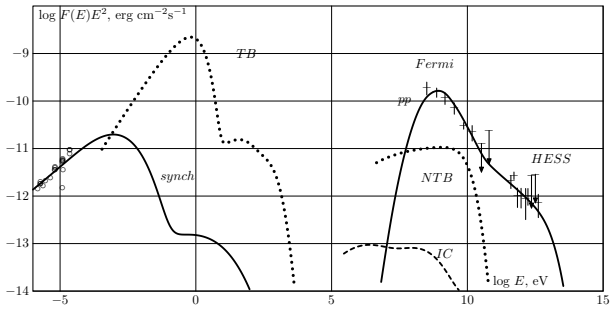


FIG. 4: The results of modeling of electromagnetic radiation of W28. The following radiation processes are taken into account: synchrotron radiation of accelerated electrons (solid curve on the left), IC emission (dashed line), gamma-ray emission from pion decay (solid line on the right), thermal bremsstrahlung (dotted line on the left), nonthermal bremsstrahlung (dotted line on the right). Experimental data in gamma-ray Fermi LAT [16]; HESS [17] (data with error-bars) and radio-bands [18] (circles) are also shown.

density n_H was adjusted to reproduce the observable gamma ray fluxes. The number density of neutrals was adjusted to reproduce the spectral shape of gamma emission. The remnant evolution was calculated up to the instant of time T when the radius of the forward shock equals to the observable radius R_f. The electron to proton ratio K_{ep} was adjusted to reproduce the observable radio-flux. The numbers in three last columns of Table I that is the age T, shock speed V_f and magnetic field strength B_f just downstream of the shock were obtained in the modeling.

Figures (1)-(5) illustrate the results of our numerical calculations.

Radial dependencies of physical quantities in SNR W28 at present ($T = 37$ kyr) are shown in Fig.1. The contact discontinuity between the ejecta and the interstellar gas is at $r = R_c = 6.6$ pc. The gas temperature drops sharply downstream of the forward shock due to the radiative cooling. However a thin dense shell is not formed because of CR pressure (cf. [6]). The central part of the remnant is filled by the hot rarefied gas with temperature $10^6 - 10^7$K.

Spectra of accelerated in W28 protons and electrons at $T = 37$ kyr are shown in Fig.2. At this point the maximum energy of accelerated protons is about 10 GeV. This value is in accordance with with the estimate of the maximum energy in the partially ionized medium $E_{\max} = u_8^3 n_H^{1/2} n_n^{-1}$ TeV [15]. For shock velocity $V_f \sim 100$ km s^{-1} that is $u_8 = 0.1$ and using the

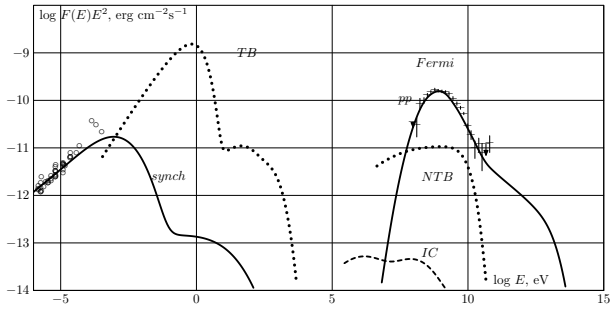


FIG. 5: The results of modeling of electromagnetic radiation of W44. The following radiation processes are taken into account: synchrotron radiation of accelerated electrons (solid curve on the left), IC emission (dashed line), gamma-ray emission from pion decay (solid line on the right), thermal bremsstrahlung (dotted line on the left), nonthermal bremsstrahlung (dotted line on the right). Experimental data in gamma-ray Fermi LAT [19], (data with error-bars) and radio-bands [20, 21] (circles) are also shown.

parameters from the Table I we indeed get $E_{\max} \sim 10$ GeV.

The spectra of particles N_{int} produced during 37 kyr after supernova explosion are shown in Fig.3. They are calculated via the integration throughout the simulation domain and via the integration on time of the outward diffusive flux at the simulation boundary at $r = 2R_f$. About 85% of the kinetic energy of explosion is transferred to cosmic rays. Most of this energy is gone by escaped particles. The maximum energy of escaped particles is 100 TeV for this SNR.

While the maximum energy of protons at the shock is about 10 GeV the interior of SNR contains protons with energies up to several TeV. They were accelerated earlier when the shock speed was higher.

Results of multi-band modeling of SNRs W28 and W44 are shown in Figures 4,5. Thermal emission shows two components. One is produced by the hot gas in the remnant interior while lower energy component is produced by the dense gas radiatively cooled and recombined behind the shock front.

IV. DISCUSSION

High acceleration efficiency (85%) in our modeling seems at odds with the lower energetics of $10 - 20\%$ expected for Galactic SNRs. Higher density of circumstellar medium might permit the lower acceleration efficiency. However this will result in the overproduction of the thermal radio emission in SNR W44. Indeed the thermal radio-flux is only slightly below than the *Planck* data [21] at high radio-frequencies (see Fig. 5). In this regard the direct DSA scenario seems more probable in comparison with the reacceleration scenario in SNR W44 [22].

The main part of gamma emission in W28 and W44 is produced by energetic protons via *pp* collisions. The gamma emission at GeV energies is produced by protons recently accelerated at the forward shock. Their energy is regulated by the neutral damping of MHD waves upstream of the shock. Higher energy gamma emission is produced by particles accelerated earlier when the shock speed was higher. The confinement of these particles is very efficient because of the Bohm like diffusion in the ionized remnant interior.

So we conclude that the neutral damping naturally results in appearance of high energy tails of gamma emission in old SNRs.

The work was supported by Russian Foundation of Fundamental Research grant 16-02-00255.

[1] Krymsky, G.F. 1977, Soviet Physics-Doklady, 22, 327
[2] Bell, A.R., 1978, MNRAS, 182, 147
[3] Axford, W.I., Leer, E. & Skadron, G., 1977, Proc. 15th ICRC, Plovdiv, 90, 937
[4] Blandford, R.D., & Ostriker, J.P. 1978, ApJ, 221, L29
[5] Lemoine-Goumard M. Proceedings of IAU Symposium 2014, 296, 287
[6] Lee S.H., Patnaude D.J., Raymond J.C. et al. 2015, ApJ 806, 71
[7] Zirakashvili, V.N. & Ptuskin V.S. 2012, Astropart. Phys., 39, 12
[8] Bell, A.R., 2004, MNRAS, 353, 550
[9] Zirakashvili, V.N., & Ptuskin, V.S., 2008, ApJ, 678, 939
[10] Bell, A.R., 2014, Astropart. Phys., 43, 56
[11] Caprioli, D., 2014, Nuclear Physics B (Proc. Suppl.), 256, 48
[12] McKenzie, J.F., & Völk, H.J., 1982, A&A, 116, 191
[13] Chevalier R. 1999, Astrophys. J. 511, 798.
[14] Reach, W.T., Rho, J., & Jarrett, T.H., 2005, ApJ 618,297
[15] Drury, L.O., Duffy, P., & Kirk, J. G. 1996, A&A, 309, 1002
[16] Abdo, A.A., Ackermann, M., Ajello, M., et al. 2010, ApJ, 718, 348
[17] Aharonian, F., et al. 2008, A&A, 481, 401
[18] Dubner, G.M., Velazquez, P.F., Goss, W.M., & Holdaway, M.A., 2000, ApJ, 120, 1933
[19] Ackermann, M., Ajello, M., Allafort, A., et al. 2013, Sci, 339, 807
[20] Castelletti1, G., Dubner, G., Brogan, C., & Kassim, N.E., 2007, A&A 471, 537
[21] Arnaud M., Ashdown M., Atrio-Barandela F. et al., 2016, A&A 586, 134
[22] Cardillo, M., Amato, E., & Blasi, P., 2016, A&A 595, 58